01 Nov 2004

Quantification of Solids Flow in a Gas-Solid Riser: Single Radioactive Particle Tracking

Satish Bhusarapu

Muthanna H. Al-Dahhan
Missouri University of Science and Technology, aldahhanm@mst.edu

Milorad P. Dudukovic

Recommended Citation

S. Bhusarapu et al., "Quantification of Solids Flow in a Gas-Solid Riser: Single Radioactive Particle Tracking," *Chemical Engineering Science*, vol. 59, no. 22 thru 23, pp. 5381 - 5386, Elsevier, Nov 2004.
The definitive version is available at https://doi.org/10.1016/j.ces.2004.07.052

ELSEVIER

Chemical Engineering Science 59 (2004) 5381–5386

Chemical Engineering Science

www.elsevier.com/locate/ces

Quantification of solids flow in a gas–solid riser: single radioactive particle tracking

Satish Bhusarapu, Muthanna Al-Dahhan, Milorad P. Dudukovic*

Chemical Reaction Engineering Laboratory, Department of Chemical Engineering,Campus Box 1198, 1 Brookings Drive, Washington University, St. Louis, MO 63130-4899 USA

Received 3 March 2004
Available online 23 September 2004

Abstract

Solids in risers of circulating fluidized beds (CFB) exhibit local backflow and recirculation. Measurement of the concentration-time response to an impulse injection of tracer, even at two elevations cannot determine the residence time distribution (RTD) of solids uniquely. Hence, evaluation of RTD in risers from conventional tracer responses is difficult and often not possible. In addition, estimating the solids circulation rate in these closed loop systems, is a non-trivial problem. In this work, a single radioactive particle in the CFB loop is tracked during its multiple visits to the riser and, by invoking ergodicity, solids circulation rate, accurate solids RTD and additional information on the solids flow pattern in the riser are estimated. A calibration curve was established for the overall solids mass flux as a function of superficial gas velocity. A second peak in the probability density function (PDF) of the solids RTD curve in the riser was observed for operating conditions in the fast-fluidization regime.

Keywords: Riser; Multiphase flow; Hydrodynamics; Residence time; Visualisation; Mixing

1. Introduction

In operation and design of circulating fluidized bed (CFB) reactors, it is important to know the total solids circulation rate, residence time distribution (RTD) of solids in various segments of the CFB loop and the flow pattern and mixing of solids in the riser. At the moment there are no reliable in situ techniques for measurement of solids circulation rates. Crude estimates are made based on measured pressure drops in the downcomer and/or riser. Tracer techniques are employed to determine the solids RTD, and many methods are used (Avidan, 1980; Bader et al., 1988; Kojima et al., 1989; Ambler et al., 1990; Patience et al., 1990; Wei et al., 1998; Harris and Davidson, 2002).

All tracer impulse response based measurements of the solids RTD have limitations, caused by (a) the choice of tracer particles, (b) the method of introducing and detecting the tracer, (c) the choice of inlet and response measurement plane for the tracer, etc. (Harris and Davidson, 2002). In systems like risers and fluidized beds where strong dispersion fluxes are present finding a true RTD with its proper mean and variance is a non-trivial matter (Nauman and Buffham, 1983). The measured impulse responses are not representative of the RTD probability density function (PDF), which requires that the system be "closed" at injection and measurement planes (i.e., at those planes convective flow should dominate). Moreover, in systems with total recirculation, like in CFBs, it is well known that the PDF of the first passage times in the riser cannot be found uniquely even from impulse response measurements at a few locations (Shinnar et al., 1971).

Various investigators often matched simple models to the observed impulse solid tracer responses and evaluated dispersion coefficients as measures of solids mixing. The experimental conditions, however, often did not satisfy the assumptions of the models and solids circulation rates were not known with certainty. This casts doubts on the

* Corresponding author. Tel.: +1-314-935-6021; fax: +1-314-935-4832.
E-mail address: dudu@wustl.edu (M.P. Dudukovic).

0009-2509/$ - see front matter © 2004 Elsevier Ltd. All rights reserved.
doi:10.1016/j.ces.2004.07.052

evaluated dispersion coefficients. Avidan (1980), Patience et al. (1990), and Rhodes et al. (1991) studied the effects of operating conditions on axial solids mixing in risers. Avidan (1980) observed a maximum in the effective axial solids dispersion coefficient as a function of gas superficial velocity and solids circulation rate and attributed this maximum to transition from turbulent to fast fluidization regime. At higher gas velocities, axial solids dispersion decreased indicating a reduction in the internal solids recirculation in the risers. Experimental results and correlation from Rhodes et al. (1991) indicate that the axial solids dispersion decreases with increasing riser diameter, supporting the notion that the annular region is in fact a wall effect. They also showed that the axial solids dispersion decreased with solids mass flux. Contrary to this result, Patience et al. (1990) found that the solids axial dispersion increased with solids mass flux. Ambler et al. (1990) found that the internal solids recirculation is greater for larger particles, while the breakthrough times, the time at which solids tracer particles are first detected at the exit, are shorter.

Numerical values of the axial dispersion coefficient D_z in risers often include the bottom zone of denser fluidized bed and are obtained by fitting the data with the simple axial dispersion model. They provide a crude measure of the extent of solids mixing in the riser. The large range of D_z values recorded (10^{-4}–$31\,m^2\,s^{-1}$) reflects the range of solid fluxes used and is due to the fact that different investigations included different mixing regions to a different extent. Experimental conditions and riser diameters also varied. Hence, the D_z values often represent the mixing averaged over the bottom zone, transition zone and the dilute zone and are influenced by the proportions of the different regions included in the measurements. The larger values of D_z ranging from 0.1 to $31\,m^2\,s^{-1}$, are likely due to the enhanced mixing in the bottom denser fluidized zone.

In this study we show that tracking a single radioactive particle which is identical in size and density to the solids in the system, one can obtain solids circulation rates, solids RTDs and additional detailed information on the solids flow pattern in the riser.

2. Experimental

The pilot plant gas–solid CFB shown in Fig. 1 was used. The total height of the glass riser is 26 ft (7.9 m) and the internal diameter is 6 in (15.2 cm). The solids are soft, approximately spherical, glass beads with a mean diameter (d_p) of 150 μm and a particle density (ρ_s) of $2550\,kg\,m^{-3}$, which fall into Group B of Geldart's classification. The secondary fluid (air) enters the system at the base of the riser, and flow is regulated by a standard air flow meter. The two phase gas–solid suspension in the riser exits into an axi-symmetric disengagement section. Air exits from the disengagement section to a cyclone, connected to the hopper at its bottom. Air from the top of the cyclone exits into a dust collector.

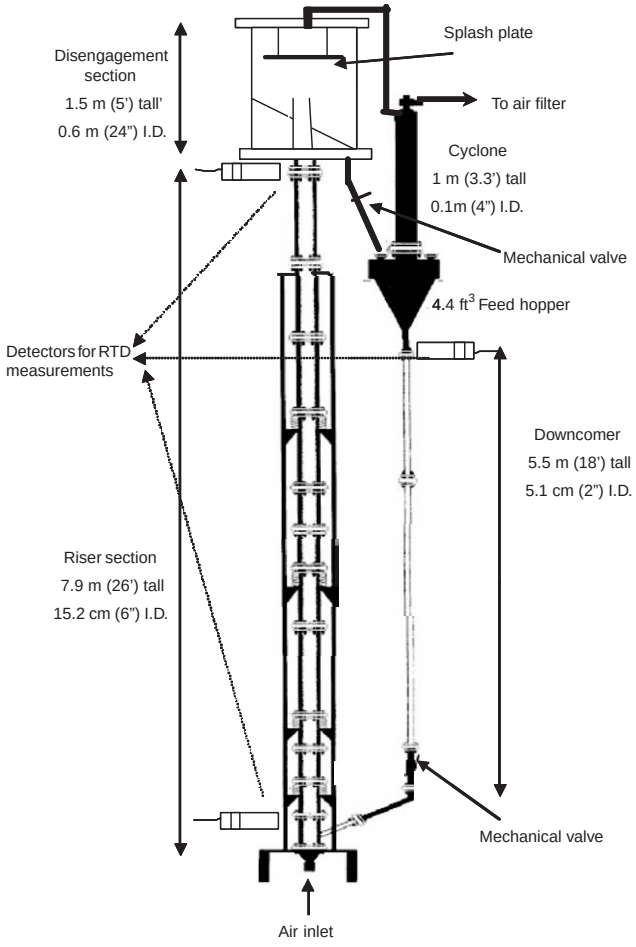

Fig. 1. Schematic diagram of the CFB setup.

The hopper is connected by a flexible pipe to the return leg (downcomer), and the solids return to the base of the riser through the downcomer. The glass downcomer is 18 ft tall with a 2 in (5.1 cm) internal diameter. The base of the downcomer is connected to the base of the riser with a 45° angled standpipe of 2 in (5.1 cm) diameter, made of glass. To regulate the flow of solids into the riser, a mechanical ball valve was placed between the base of the downcomer and the 45° standpipe.

2.1. Tracer studies

A single radioactive particle (^{46}Sc) was used as a tracer. It was tailored by coating a layer of polymer (Parylene N) on the Scandium particle to achieve the same density as the solids used (glass beads) and the same diameter (150 μm) as the mean particle size of glass beads. By tracking this single radioactive tracer at a data acquisition frequency of 200 Hz and in different sections along the CFB loop, following measurements were made: (a) overall solids mass flux, (b) solids RTD for the entire riser, and (c) instantaneous solids velocity field in a developed flow section. Only the

Table 1
Operating conditions and regimes for solids RTD measurements

U_g^{riser} (m s^{-1})	3.2	3.9	4.5
G_s (kg m^{-2} s^{-1})	26.6 ± 1.1	30.1 ± 0.8	32.1 ± 1.3
$Ar^{1/3}$, V^*, regime	(6.9,4.73,FF)	(6.9,5.7,DPT)	(6.9,6,DPT)
G_s (kg m^{-2} s^{-1})	30.1 ± 1.1	33.7 ± 1.2	36.8 ± 0.9
$Ar^{1/3}$, V^*, regime	(6.9,4.7,FF)	(6.9,5.4,DPT)	(6.9,5.7,DPT)

FF—Fast Fluidization, DPT—Dilute Phase Transport, $Ar = \rho_g(\rho_p - \rho_g)d_p^3 g/\mu_g^2$ and $V^* = \left[\frac{\rho_g^2}{g\mu_g(\rho_p-\rho_g)}\right]^{1/3}\left[U_g^{\text{riser}} - \frac{G_s\varepsilon}{\rho_p(1-\varepsilon)}\right]$.

first two results are discussed here. The experimental conditions included three different superficial gas velocities varying from 3.2 to 4.5 m s^{-1} and two different solids loading of 140 and 190 lbs at ambient pressure and temperature. This spans from fast fluidization (FF) to dilute phase transport (DPT) operating regimes indicated in Table 1.

2.1.1. Overall solids mass flux measurements

The measurement consists of: (i) tracking a single radioactive tracer particle by using two NaI (Tl) scintillation detectors to estimate the solids velocity and (ii) measuring the solids holdup in the same section by γ-ray line densitometry. By representing both the solids velocity and holdup by the sum of deterministic and fluctuating components, and given a cross-sectional area (A) of the section, the ensemble averaged solids mass flux $\langle G_s \rangle$ in the section can be obtained as

$$\langle G_s \rangle = \frac{\rho_s}{A}\left[\int_A \langle v_s \rangle \cdot \langle \varepsilon_s \rangle \, \mathrm{d}A + \int_A \langle v_s' \varepsilon_s' \rangle \, \mathrm{d}A\right], \quad (1)$$

$$\langle G_s \rangle \approx \frac{\rho_s}{A}\int_A \langle v_s \rangle \cdot \langle \varepsilon_s \rangle \, \mathrm{d}A \approx \rho_s \cdot \langle v_s \rangle \cdot \langle \bar{\varepsilon}_s \rangle. \quad (2)$$

The following assumptions are needed to arrive at Eq. (2): (1) $\varepsilon_s'(t)$ and $v_s'(t)$ profiles are uncorrelated over the whole cross section, (2) they are averaged values, (3) $\langle v_s \rangle \neq f(r, \theta)$, and (4) $\langle \varepsilon_s \rangle \neq f(r, \theta)$. Essentially plug flow condition for solids in the cross section of interest is required. The downcomer section (2 in column) of the CFB loop was used, since it was observed during operation that this section was always filled with a bed of solids moving in a state close to a packed bed. Overall solids mass flux is obtained as a function of solids inventory and superficial gas velocity as shown in Table 1. Further details of the technique and results can be found in Bhusarapu et al. (2004).

2.1.2. Solids RTD measurements

Three shielded detectors, used for tracking the particle (as indicated in Fig. 1), were placed in the loop: (i) at the base of the riser, at 5″ above the solids entry zone into riser, and 15″ above the air entry; (ii) at the riser exit, 3″ below the disengagement section; (iii) at the start of the downcomer, 10″ below the hopper section. Tracking a single radioactive tracer during its multiple visits along the loop is equivalent to tracking "all" the solids in the loop. The time spent by the tracer between the cross-sectional planes of the detectors can be found and represents the residence times in the riser, disengagement and hopper, and downcomer. Thus, in this method, which is non-invasive, the problem of introducing and detecting the tracer is eliminated, and no artificial experimental boundary conditions need to be imposed. In fact, true "open–open" boundaries of the system remain undisturbed. Since only a single tracer particle is being tracked, a new challenge arises in obtaining the precise "time of passage" of the tracer at the cross sectional planes of the detectors.

Fig. 2a shows the schematic of a typical trajectory of the tracer particle in the riser. In systems such as CFB, where backflow is significant, especially at the inlet (bottom) of the riser, the tracer particle might pass back and forth across the plane of the detector at the inlet many times before it flows through the riser to be detected by the detector above the riser at the exit plane. Hence, we can expect to have many peaks in the detector response as the tracer particle passes the detector plane. This is shown in Fig. 2b, which displays a part of the raw data from the detectors located at the riser inlet, exit and top (entry) of the downcomer. The time elapsed between spikes recorded at different detectors allows us to determine whether the tracer passed the inlet detector several times entering and exiting the system at the inlet, or whether it passed the detector at the riser exit after passing by the inlet detector. The different magnitude of the spikes detected (see Fig. 2b) indicates that the tracer crossed the detector plane at different distances from the detector face. In order to ensure that the detectors view only the cross-sectional plane of interest, they were heavily shielded by wrapping the column above and below the cross-section with lead sheet. Therefore, by counting in pairs, the entry and exit of the tracer into the system (region of the riser between the cross-sectional planes viewed by the detectors), we can precisely calculate the time that the tracer particle spent inside the system and outside the system. For example, in the typical trajectory shown in Fig. 2a, the tracer enters the system at point A, corresponding to spike 1 in Fig. 2b, then exits at point B at the same plane, corresponding to spike 2, and finally re-enters the system again at C, corresponding to spike 3. Hence, the time spent by the tracer between positions B and C should not be counted as residence time in the riser and only the time spent between A and B and between C and D is taken as the residence time. The same approach is applied near the exit of the riser at the cross-sectional plane D. In this way, we can accurately estimate the RTD of the solids in the riser.

It should be noted that the data obtained from single particle tracking is rich. One can precisely derive not only the distribution of total residence time in the system, but also the distribution of first passage times (in at the inlet–out at the exit). Moreover, one can directly evaluate a macromixing index based on Trajectory Length Distribution (TLD) and other mixing parameters such as return length and

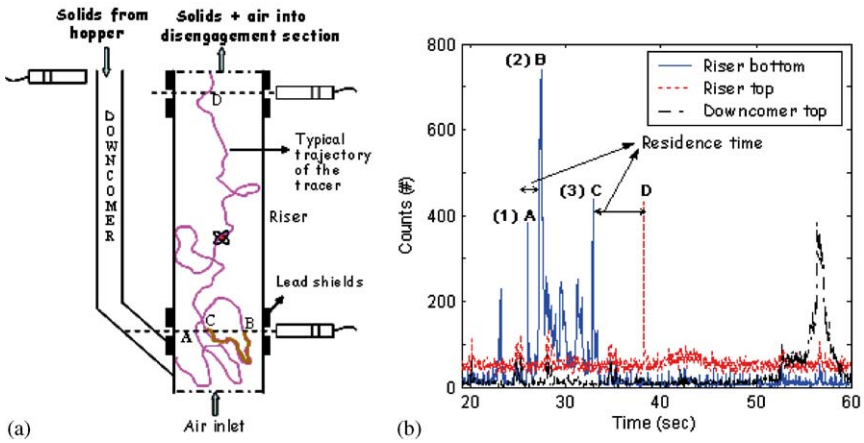

Fig. 2. (a) Schematic of the three detectors along the CFB loop with a typical trajectory; (b) Part of the raw data obtained from the three detectors.

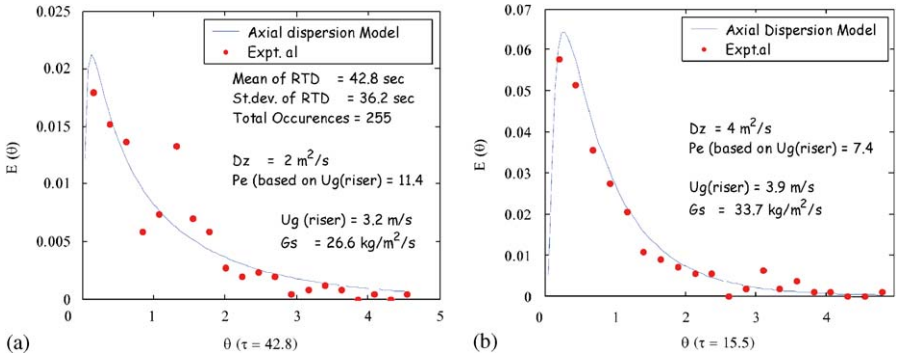

Fig. 3. Experimental and simulated solids RTD in the riser at: (a) $U_g^{\text{riser}} = 3.2\,\text{m s}^{-1}$ and G_s of $26.6\,\text{kg m}^{-2}\,\text{s}^{-1}$; (b) $U_g^{\text{riser}} = 3.9\,\text{m s}^{-1}$ and G_s of $33.7\,\text{kg m}^{-2}\,\text{s}^{-1}$.

circulation time distribution, as proposed by Villermaux (1996). In addition, Cycle Time Distribution (CTD) can also be estimated from the data. CTD is defined as the time elapsed between consecutive passages of a certain fluid element past the cross section through which all the fluid passes (Mann and Crosby, 1973).

3. Results and discussion

Fig. 3a shows the PDF of the residence times of the tracer inside the riser section of the loop at a superficial gas velocity (U_g^{riser}) of $3.2\,\text{m s}^{-1}$ and solids mass flux (G_s) of $26.6\,\text{kg m}^{-2}\,\text{s}^{-1}$, which corresponds to the FF regime. The mean (τ) and standard deviation of the RTD are 42.8 and 36.2 s, respectively. The occurrence of the second peak in the RTD curve is suggested at 1.2 τ. The PDF of the RTD curve has a long tail, which is a typical characteristic of a system with internal recirculation. By ignoring the possibility of the second peak and by fitting the data with a simple axial dispersion model (ADM), the axial dispersion coefficient, D_z, was found to be $2\,\text{m}^2\,\text{s}^{-1}$ and the dimensionless Peclet number (Pe) based on superficial gas velocity in the riser (U_g^{riser}) is 11.4. Also, Peclet number based on solids superficial velocity (Pe_s), obtained from τ, was found to be 0.6. Clearly, ADM model can never predict a second peak in the RTD curve. Low value of Pe_s raises doubts about the use of ADM.

Fig. 3b shows a comparison of the experimental PDF of the RTD and a fitted ADM model at a superficial gas velocity in the riser of $3.9\,\text{m s}^{-1}$ and solids mass flux of $33.7\,\text{kg m}^{-2}\,\text{s}^{-1}$ corresponding to the DPT regime. At this condition, the total number of tracer particle visits was 277 which is equivalent to introducing 277 tagged tracer particles. The second peak cannot be seen, although the E-curve has a long tail. The dispersion coefficient (D_z) was found to be $4\,\text{m}^2\,\text{s}^{-1}$ and the Peclet numbers based on the gas superficial velocity and on the solids superficial velocity in the riser are 7.4 and 0.8, respectively. The ADM seems to fit the data well.

To check the reproducibility, solids RTD data was obtained with another similar tracer particle with fresh solids inventory at the identical operating conditions ($U_g^{\text{riser}} = 3.2\,\text{m s}^{-1}$, $G_s = 26.6\,\text{kg m}^{-2}\,\text{s}^{-1}$; $U_g^{\text{riser}} = 3.9\,\text{m s}^{-1}$, $G_s = 33.7\,\text{kg m}^{-2}\,\text{s}^{-1}$). Figs. 4a and b show the solids RTDs and the E-curve obtained after a longer data acquisition with

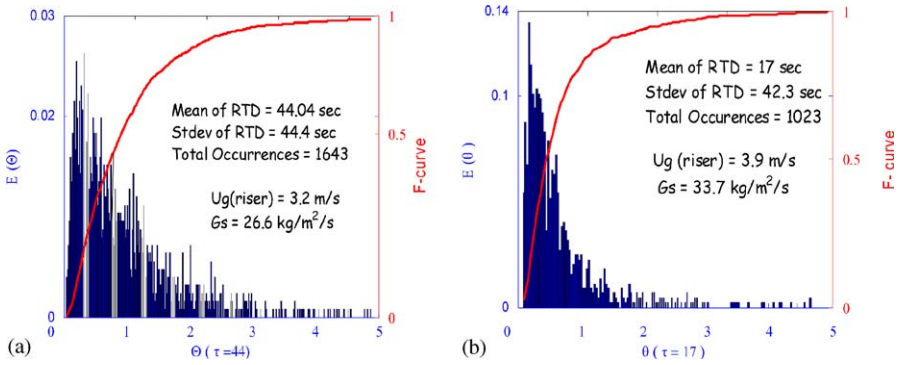

Fig. 4. Solids RTD and its cumulative distributions at U_g^{riser} and G_s of: (a) 3.2, 26.6; (b) 3.9, 33.7. Note that abscissas for each plot are different.

higher number of occurrences for each of the conditions. Percentage difference in the mean residence times obtained from the repeated experiments was 2.8% and that of the dispersion coefficients was 5%. This confirms that solids RTD experiments are reproducible within engineering accuracy. To validate the assumption of ergodicity, mean residence times at a given operating condition were examined as a function of total tracer occurrences. For all the experimental conditions the mean residence time converges to within the 95% confidence interval after about 300 occurrences except at $U_g^{\text{riser}} = 3.9\,\text{m s}^{-1}$ and $G_s = 33.7\,\text{kg m}^{-2}\,\text{s}^{-1}$, when about 1000 occurrences are needed. Hence, the presented RTDs are number of occurrences independent.

Overall solids holdup ($\varepsilon_s^{\text{overall}}$) in the riser can be obtained from the knowledge of the mean residence time (τ) and overall solids mass flux (G_s). $\varepsilon_s^{\text{overall}}$ value of 6% is obtained at $U_g^{\text{riser}} = 3.2\,\text{m s}^{-1}$ and $G_s = 26.7\,\text{kg m}^{-2}\,\text{s}^{-1}$, which is a typical FF regime holdup. A value of 3% is found at $U_g^{\text{riser}} = 3.9\,\text{m s}^{-1}$ and $G_s = 33.7\,\text{kg m}^{-2}\,\text{s}^{-1}$, which is close to the DPT regime holdup (<2%). The ratio of $\varepsilon_s^{\text{overall}}$ for the two operating conditions, shows that for the condition in the DPT regime, there were 49% of solids that were in the condition in FF regime. To look at the overall flow patterns in these two regimes, moments of the RTD curve were evaluated. Referring to Fig. 4, dimensionless variance of 1 was obtained for the operating condition in the FF regime, indicating that the solids flow in the riser (as far as the variance is concerned) is close to a stirred tank. However, the dimensionless variance for the DPT regime is 6.2, indicating the existence of either stagnant zones or bypassing, or both.

In examining the solids RTD (F-curves), smaller slopes are observed on the dimensionless time scale when an indication of a second peak is seen in the PDF curve. Absence of the second peak and rapid rise of the RTD (high slope) seem to be indicative of dilute transport (refer to Table 1), where the slip velocity between the gas and solids tends to be small and close to the terminal velocity of the particles. In contrast, solids flow pattern in Fig. 4a is in the fast-fluidization regime. Similar results were observed at the other conditions which are not shown here for brevity. Thus, the shape of the RTD seems to be indicative of the flow regime.

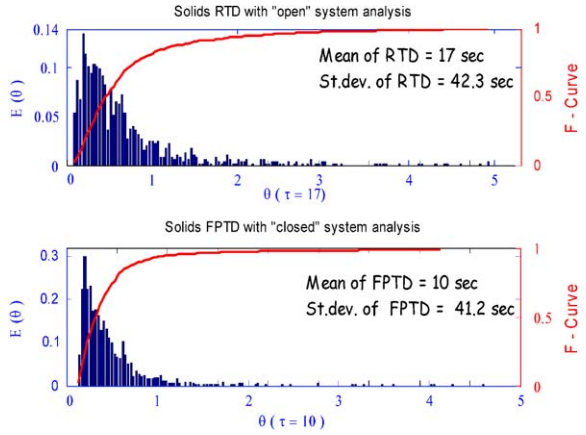

Fig. 5. Comparison of the solids RTD and FPTD curves for the entire riser at $U_g^{\text{riser}} = 3.9\,\text{m s}^{-1}$ and $G_s = 33.7\,\text{kg m}^{-2}\,\text{s}^{-1}$ obtained with "open" and "closed" system analysis, respectively.

Single particle tracking in systems with high backmixing, like the gas–solid riser with "open–open" boundaries allows us to interpret the detector responses in different ways. For example, two different distributions are readily obtained. One is the distribution of total residence times in the system (RTD). The other, the distribution of sojourn times for the first passage of particles that go directly from the inlet to the exit plane, is named first passage time distribution (FPTD). In other words, true solids RTD results by allowing for "open–open" boundaries of the system, while solids FPTD is obtained by imposing "closed–closed" boundaries. The method for data analysis to derive the solids RTD was described in the previous section.

Plots in Fig. 5 show the histograms of the occurrences and the cumulative occurrences (proportional to F-curve) versus time for total residence time and first passage times. The means of the RTD and FPTD are quite different, with a difference of 41%, while there is only a 3% difference in the standard deviations. Lower mean of FPTD as compared to RTD is expected since the first passage time will represent the time elapsed between the final entry at the inlet plane (with no return) to the first exit at the exit plane.

However, dimensionless variance for FPTD, calculated to be 17, is much larger than that of the RTD (6.2), indicating an enormous bypassing in the riser. Hence, from the ratio of the means of RTD (17 s) to FPTD (10 s), shows that 59% of the solids travel from inlet to exit in a single pass without re-exiting at the inlet. However, they exhibit a large dimensionless variance, which means that few solids go out fast and straight through the riser while the rest recirculate internally in the riser by slipping down and rising and skipping, etc. Hence, our data establish that 41% of the solids in the riser at DPT condition re-exit at the entry and keep re-entering. This value is of interest for modeling FCC risers. The dispersion coefficient calculated for FPTD (Fig. 5) was found to be $7.3\,m^2\,s^{-1}$, which is 83% higher than the dispersion coefficient obtained for RTD. Hence, grossly overestimated values are obtained if D_z from FPTD is used to characterize the axial dispersion in risers. Moreover, if a bundle of tracer particles were to be injected at the bottom of the riser and their concentration measured at the exit, the obtained response will not be either the shown RTD, or the FPTD, but a distribution of some other travel time of the solids. Hence, conventional tracer injection techniques, with controlled boundaries ("closed–closed") can at best provide a FPTD, which overestimates the dispersion coefficients.

4. Summary

Solids mixing in a gas–solid riser was investigated by tracking a single radioactive tracer particle. The assumption of ergodicity underlying the experiments was corroborated and true solids residence times and first passage times were estimated. It was established for the operating condition in the DPT regime that 59% of the solids travel from inlet to exit in a single pass without re-exiting at the inlet. Dispersion coefficients obtained from FPTD overestimates the axial dispersion in risers. Dual peaks were seen in the PDF of the solids RTD for the experimental conditions in the fast-fluidization regime, but not in the dilute transport regime.

Notation

A	mean cross-sectional area, m^2
Ar	Archimedes number, $\rho_g(\rho_p-\rho_g)d_p^3 g/\mu_g^2$
d_p	particle diameter, m
D	dispersion coefficient, $m^2\,s^{-1}$
G_s	mass flux, $kg\,m^{-2}\,s^{-1}$
Pe	Peclet number
U_g^{riser}	superficial gas velocity, $m\,s^{-1}$
V^*	dimensionless net superficial gas velocity $\left[\frac{\rho_g^2}{g\mu_g(\rho_p-\rho_g)}\right]^{1/3}\left[U_g^{\text{riser}}-\frac{G_s\varepsilon}{\rho_p(1-\varepsilon)}\right]$
E	PDF of RTD (dimensionless)

Greek letters

$\bar{\varepsilon}_s$	mean of the line-averaged solids volume fraction (dimensionless)
ε_s'	fluctuating component of the line-averaged solids volume fraction
v_s	solid phase velocity in axial direction, $m\,s^{-1}$
$\langle v_s\rangle$	ensemble averaged velocity of the solids phase, $m\,s^{-1}$
v_s'	fluctuating component of the solids phase velocity, $m\,s^{-1}$
ρ	density, $kg\,m^{-3}$
τ	mean residence time, s
θ	dimensionless time

Subscripts

s	solid phase
z	axial
r	radial

Acknowledgements

The authors would like to thank DOE-OIT for sponsoring the work, DuPont for his help during the CFB experimental setup, Dr. Pascal Fongarland for his help in the CFB setup, Sandia National Laboratory for their technical support, and MIT Nuclear Reactor Laboratory for irradiating the radioactive particle.

References

Ambler, P.A., Milne, B.J., Berruti, F., Scott, D.S., 1990. Chemical Engineering Science 45 (8), 2179–2188.
Avidan, A.A., 1980. Ph.D. Dissertation, The City College, New York.
Bader, R., Findlay, J., Knowlton, T.M., 1988. In: Basu, P., Large, J.F. (Eds.), Circulating Fluidized Bed Technology II. Pergamon Press, New York, pp. 123–137.
Bhusarapu, S., Fongarland, P., Al-Dahhan, M.H., Dudukovic, M.P., 2004. Powder Technology, accepted.
Harris, A.T., Davidson, J.F., 2002. Chemical Engineering Journal 89, 127–142.
Kojima, T., Ishihara, K., Guittlin, Y., Furusawa, T., 1989. Journal of Chemical Engineering of Japan 22, 341–346.
Mann, U., Crosby, E.J., 1973. Chemical Engineering Science 28, 623–627.
Nauman, E.B., Buffham, B.A., 1983. Mixing in continuous flow systems, Wiley, New York, (Chapter 3).
Patience, G.S., Chaouki, J., Kennedy, G., 1990. In: Basu, P., Horio, M., Hasatani, M. (Eds.), Circulating Fluidized Bed Technology III. Pergamon Press, New York, pp. 627–632.
Rhodes, M.J., Zhou, S., Hirama, T., Cheng, H., 1991. A.I.Ch.E. Journal 1450–1458.
Shinnar, R., Naor, P., Katz, S., 1971. Chemical Engineering Science 27 (9), 1627–1642.
Villermaux, J., 1996. Chemical Engineering Science 51 (10), 1939–1946.
Wei, F., Cheng, Y., Jin, Y., Yu, Z., 1998. The Canadian Journal of Chemical Engineering 76, 19–26.